2014 IEEE International Conference on Robotics & Automation (ICRA)
Hong Kong Convention and Exhibition Center
May 31 - June 7, 2014. Hong Kong, China

# Accurate target tracking control for a mobile robot: a robust adaptive approach for off-road motion

Roland Lenain[1], Benoit Thuilot[2,3], Audrey Guillet[1], Bernard Benet[1]

[1] Irstea, 24 avenue des Landais, 63172 Aubière, France

[2] Clermont Université, Université Blaise Pascal, Institut Pascal, BP 10448, 63000 Clermont-Ferrand, France

[3] CNRS, UMR 6602, Institut Pascal, 63177 Aubière, France

firstname.lastname@irstea.fr benoit.thuilot@univ-bpclermont.fr

***Abstract*— In this paper a control strategy for a mobile robot enabling to track a manually driven vehicle or a moving target is proposed in the context of natural environment. In such a context, the motion does not meet classical assumptions usually proposed for mobile robots, since the terrain geometry is not necessarily flat and wheels are subject to sliding. As a result, in order to preserve the accuracy of tracking, it appears necessary to account for such phenomena in the control law. Several observer-based approaches have already been developed in the framework of path following in off-road conditions, but suffer from several limitations. In particular, the velocity should not be null, which appears to be an important drawback in the proposed application: the tracking of a non-autonomous vehicle indeed imposes possible stops. In this paper, a new observation strategy is proposed allowing to avoid non-observable situations (null velocity). This permits to achieve an accurate vehicle tracking whatever its velocity, its trajectory and the grip conditions.**

## I. INTRODUCTION

Several off-road applications require to control a vehicle with a high accuracy level in harsh conditions. From defense to agriculture, the driving task in natural environment has to be addressed. Such a task may be difficult, painful, or dangerous for human drivers. The development of autonomous or semi-autonomous mobile robots may then be of interest to achieve surveillance, transportation or agriculture treatment [2]. For instance, the tracking of a moving target (such as a manually driven vehicle) may increase the efficiency of the task achieved, while still letting the leading role to the human. Path following or target tracking have been deeply theoretically studied for several types of mobile robots [7], based on an ideal modeling (rolling without sliding) of the robot motion [3]. This leads to satisfactory results when moving on urban ground at low speed, but appears to be inaccurate when achieving motions on slippery ground [5]. As a consequence, for high accurate motion servoing in natural environments or in harsh conditions, robust control with respect to low and varying grip conditions has to be developed. Several approaches have been proposed in the framework of path following, considering sliding as a perturbation to be rejected [1], and relying for instance on sliding mode control techniques [6]. These approaches avoid the modeling of grip conditions, but may appear to be conservative. Model-based adaptive approaches have also been previously proposed [4], considering an extended kinematic model. Nevertheless, an observability condition imposes a strictly positive velocity for the estimation of sideslip angles, representative of sliding effects. If it is a basic assumption in the path following task, the moving object tracking application may in contrast require to stop the robot, as the target does. The observer has then to be frozen when the speed is below a given threshold, leading to chattering effects or initialization troubles when the robot restarts, as it is highlighted in the following.

In this paper, a new adaptive approach is proposed [1]. It permits an on-line estimation of sideslip angles independently from the robot velocity. As a consequence, the extended model can always be properly adapted in order to account for sliding effects and their variation. Control is then designed to follow the trajectory of a moving object at a certain distance with a possible desired lateral offset. Since a kinematic structure of the adapted model is preserved, the lateral and longitudinal motions of the mobile robot are considered independently. A velocity control law is first derived to ensure a desired curvilinear distance to the target. A steering angle law is then defined, based on the exact linearization of the model to ensure an accurate tracking error with respect to the desired lateral distance to the trajectory.

The paper is decomposed as follows. First, the extended model is recalled from previous work, in the framework of target tracking. In a second part, the proposed observer is detailed, allowing an accurate description of the robot motion. As a relevant model is then available, the velocity and steering angle control laws are detailed in a third part. The efficiency of the approach, and the effective contributions of the paper are then investigated through full scale experiments.

## II. MODELING

### A. Mobile robots formation modeling

The objective of the control approach is to track the trajectory of a manually driven vehicle moving ahead the

[1]This work has received the support of French National Research Agency under the grant number ANR-11-ASTR-0038 attributed to Baudet-Rob project. It has also been sponsored through the RobotEx Equipment of Excellence (ANR-10-EQPX-44), by the European Union through the program Regional competitiveness and employment 2007-2013 (ERDF Auvergne rgion), and by the Auvergne region.

mobile robot, with a desired relative position (curvilinear distance and lateral offset). In this paper, the mobile robot is a car-like vehicle, considered as a bicycle (such as depicted in Figure 1). Since the objective is the tracking of the first vehicle trajectory (the successive points of the leader are approximated by second order polynomials), the motion of the robot is referred to this trajectory denoted $\Gamma$. Based on this assumption, the state variables for the robot are:

- the robot curvilinear abscissa $s$ along $\Gamma$. It represents the curvilinear distance between the initial leader's position and the closest point belonging to $\Gamma$ from point $O$, middle of the robot rear axle. Similarly, $s_L$ is the curvilinear abscissa of the leader, equal to the distance it has travelled.
- the robot tracking error $y$, which is the lateral deviation between the robot position (centre of the rear axle $O$) and the closest point to $O$ belonging to $\Gamma$ (denoted by the curvilinear abscissa $s$).
- the robot angular deviation $\tilde{\theta}$, which is the difference between absolute robot heading and the orientation of tangent to $\Gamma$ at $s$.

This type of model is commonly used in the framework of mobile robotics [9], but generally assume that the robot wheels satisfy rolling without sliding conditions. The off-road context addressed in this paper does not satisfy such conditions, and the accuracy is depreciated when using a control based on such a model in natural environment.

In order to account for non-ideal grip conditions in mo-

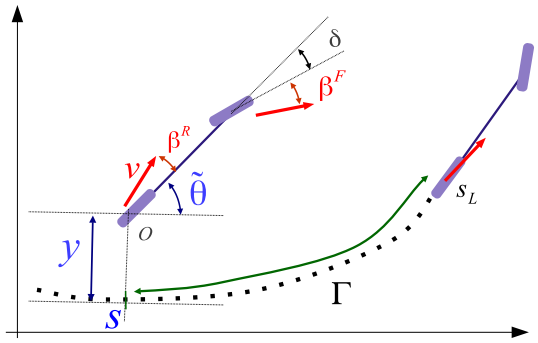


Fig. 1. Model of formation motion with one vehicle and one mobile robot

tion model, without considering the numerous parameters required by a dynamical model, two additive variables $\beta^F$ and $\beta^R$ (for front and rear axle) are introduced, see Figure 1. Named as sideslip angles, they are representative of the angles between tire orientation and actual speed vector orientation at contact points and permit to account for the influence of sliding.

### B. Motion equations

The robot motion is achieved thanks to the control variables $v$ (the vehicle velocity at point $O$) and $\delta$ (the front steering angle). Considering the actual speed vectors (accounting for sideslip angles) and with $L$ denoting the robot wheelbase, the derivative of the state variables may be computed similarly to classical kinematic models (see [4]) and leads to:

$$\begin{cases} \dot{s} &= v\frac{\cos(\tilde{\theta}+\beta^R)}{1-c(s)\,y} \\ \dot{y} &= v\sin(\tilde{\theta}+\beta^R) \\ \dot{\tilde{\theta}} &= v\left[\cos(\beta^R)\lambda_1-\lambda_2\right] \end{cases} \quad (1)$$

with : $\lambda_1 = \frac{\tan(\delta+\beta^F)-\tan(\beta^R)}{L}$, $\lambda_2 = \frac{c(s)\cos(\tilde{\theta}+\beta^R)}{1-c(s)\,y}$ where $c(s)$ is the reference path curvature at the curvilinear abscissa $s$. This model exists under the hypothesis that $1-c(s)\,y \neq 0$. This means that the point $O$ (center of rear axle) is not superimposed with the center of $\Gamma$ at $s$. This case is never encountered in practice, assuming that the robot is properly initialized.

## III. Sideslip angles estimation

### A. Observer equations

In order to derive control laws for path following and distance servoing based on the model (1), the knowledge of relevant values for sideslip angles $\beta^F$ and $\beta^R$ is mandatory. Since there is no available sensor enabling the direct measurement of such variables, an indirect estimation has to be achieved. As pointed out in [4], if a measurement of the vector $[s, y, \tilde{\theta}]$ is available (quite standard in mobile robot applications), then the sideslip angles are observable from model (1) and an indirect measurement algorithm, based on the duality between observation and control, has been proposed. Nevertheless, such an observer, named Control Based Observer (CBO) in the sequel, involves a division by the robot velocity, thus bringing to a singularity if the robot stops. Since only path following was previously addressed, the robot velocity was not supposed to be small, and if for any reason the robot velocity decreased below some threshold ($0.5m.s^{-1}$), the estimation process was stopped and reinitialized when the robot was restarting. However, if manually driven vehicle tracking is now considered, potential stops or slow motions have to be considered and CBO observer may then lead to inaccuracies (as pointed out in results section). A new observation strategy is then proposed in this paper, using an adaptation law without any restriction on the robot velocity.

In order to proceed the indirect estimation of sideslip angles, let us consider the state space model (2)

$$\dot{\xi} = \begin{bmatrix} \dot{\xi}_{dev} \\ \dot{\xi}_{\beta} \end{bmatrix} = \begin{bmatrix} f(\xi_{dev}, \xi_{\beta}, v, \delta) \\ 0_{2\times 1} \end{bmatrix} \quad (2)$$

where $\xi$ is split into two sub-states:

- $\xi_{dev} = [y\ \ \tilde{\theta}]^T$, which constitutes the deviations of the robot with respect to the trajectory $\Gamma$ (on-line defined by the leading vehicle).
- $\xi_{\beta} = [\beta^F\ \ \beta^R]^T$, which is composed of the sideslip angles, to be estimated.

In state space model (2), $f(\xi_{dev}, \xi_{\beta}, v, \delta)$ is deduced directly from the two last lines of model (1). In this formalism, only $\xi_{dev}$ is supposed to be measured and the objective is

to find an observed state $\hat{\xi}$ which converges to the actual one $\xi$, thanks to the observation error on the "deviation" part $\tilde{\xi}_{dev} = \xi_{dev} - \hat{\xi}_{dev}$. The sub-state $\hat{\xi}_\beta$ thus obtained can then be regarded as a relevant estimation of sideslip angles.

Since there is no equation attached to sideslip angles evolution, the observer is also separated into two sub-states. It has then the general form :

$$\left\{ \begin{array}{rcl} \dot{\hat{\xi}}_{dev} & = & f(\xi_{dev}, \hat{\xi}_\beta, v, \delta) + \alpha_{dev}(\tilde{\xi}_{dev}) \\ \dot{\hat{\xi}}_\beta & = & \alpha_\beta(\tilde{\xi}_{dev}) \end{array} \right. \tag{3}$$

where $\alpha_{dev}$ and $\alpha_\beta$ are functions of the observation error attached to the deviation part of the state $\xi$. Only the observation error attached to robot deviation may indeed be known, while the sideslip angles observation error, denoted hereafter $\tilde{\xi}_\beta = \xi_\beta - \hat{\xi}_\beta$, cannot be evaluated. As a result, the function $f$ used in observer (3) takes as parameters the actual (i.e. measured) sub-state $\xi_{dev}$ but only the estimated sideslip angles $\hat{\xi}_\beta$.

The objective is then to find functions $\alpha_{dev}$ and $\alpha_\beta$ allowing the convergence of both $\tilde{\xi}_{dev}$ and $\tilde{\xi}_\beta$ to zero. The observation error dynamics indeed depends on these two functions as their expressions are:

$$\left\{ \begin{array}{rcl} \dot{\tilde{\xi}}_{dev} & = & f(\xi_{dev}, \xi_\beta, v, \delta) - f(\xi_{dev}, \hat{\xi}_\beta, v, \delta) - \alpha_{dev}(\tilde{\xi}_{dev}) \\ \dot{\tilde{\xi}}_\beta & = & -\alpha_\beta(\tilde{\xi}_{dev}) \end{array} \right. \tag{4}$$

Considering the linearization of function $f(\xi_{dev}, \xi_\beta, v, \delta)$ around the estimated sideslip angles $\hat{\xi}_\beta$, one can rewrite $f$ as follows:

$$\begin{array}{rcl} f(\xi_{dev}, \xi_\beta, v, \delta) & = & f(\xi_{dev}, \hat{\xi}_\beta, v, \delta) + \frac{\partial f}{\partial \xi_\beta}(\xi_{dev}, \hat{\xi}_\beta, v, \delta)\tilde{\xi}_\beta \\ & & + O(\tilde{\xi}_\beta{}^2) \end{array} \tag{5}$$

which leads to the following observation error dynamics:

$$\left\{ \begin{array}{rcl} \dot{\tilde{\xi}}_{dev} & = & \frac{\partial f}{\partial \xi_\beta}(\xi_{dev}, \hat{\xi}_\beta, v, \delta)\, \tilde{\xi}_\beta - \alpha_{dev}(\tilde{\xi}_{dev}) \\ \dot{\tilde{\xi}}_\beta & = & -\alpha_\beta(\tilde{\xi}_{dev}) \end{array} \right. \tag{6}$$

*Proposition:*
Considering the error dynamics (6), the expression (7) for the functions $\alpha_{dev}$ and $\alpha_\beta$ together with observer (3) ensures the convergence of $\tilde{\xi}$ to $0_{4\times 1}$ and then the relevant estimation of sideslip angles $(\beta^F, \beta^R)$:

$$\left\{ \begin{array}{rcl} \alpha_{dev}(\tilde{\xi}_{dev}) & = & K_{dev}\, \tilde{\xi}_{dev} \\ \alpha_\beta(\tilde{\xi}_{dev}) & = & K_\beta \left[ \frac{\partial f}{\partial \xi_\beta}(\xi, \hat{\xi}_\beta, v, \delta) \right]^T \tilde{\xi}_{dev} \end{array} \right. \tag{7}$$

with $K_{dev}$ a $2 \times 2$ positive diagonal matrix and $K_\beta$ a positive scalar. The function $\frac{\partial f}{\partial \xi_\beta}$ (partial derivative of $f$ with respect to sideslip angles) may easily computed from the expression of the extended kinematic model (1).

### B. Sketch of proof

Let us consider the candidate Lyapunov function $V$ depending on the whole observation error as:

$$V = \tfrac{1}{2} K_\beta \tilde{\xi}_{dev}^T \tilde{\xi}_{dev} + \tfrac{1}{2} \tilde{\xi}_\beta^T \tilde{\xi}_\beta \tag{8}$$

The derivative of the positive function $V$ along the solutions of system (6) has the following expression:

$$\begin{array}{rcl} \dot{V} & = & K_\beta \left[ \frac{\partial f}{\partial \xi_\beta}(\xi_{dev}, \hat{\xi}_\beta, v, \delta)\, \tilde{\xi}_\beta - \alpha_{dev}(\tilde{\xi}_{dev}) \right]^T \tilde{\xi}_{dev} \\ & & - \tilde{\xi}_\beta^T\, \alpha_\beta(\tilde{\xi}_{dev}) \end{array} \tag{9}$$

Replacing $\alpha_{dev}(\tilde{\xi}_{dev})$ and $\alpha_\beta(\tilde{\xi}_{dev})$ by their chosen expressions (7) leads to:

$$\dot{V} = K_\beta \left[ \frac{\partial f}{\partial \xi_\beta}\, \tilde{\xi}_\beta - K_{dev}\, \tilde{\xi}_{dev} \right]^T \tilde{\xi}_{dev} - K_\beta\, \tilde{\xi}_\beta^T \left[ \frac{\partial f}{\partial \xi_\beta} \right]^T \tilde{\xi}_{dev} \tag{10}$$

After simplifications, the derivative of $V$ with respect to time is equal to:

$$\dot{V} = -K_\beta\, K_{dev}\, \tilde{\xi}_{dev}^T\, \tilde{\xi}_{dev} \tag{11}$$

which is negative and moreover implies that $\tilde{\xi}_{dev}$ converges to 0. Next, injecting $\tilde{\xi}_{dev} = 0$ in the first equation (6) establishes that $\frac{\partial f}{\partial \xi_\beta}(\xi_{dev}, \hat{\xi}_\beta, v, \delta)\, \tilde{\xi}_\beta$ converges to 0 and it can eventually be inferred that $\tilde{\xi}_\beta$ converges to 0 since straightforward computations show that:

$$\det\left( \frac{\partial f}{\partial \xi_\beta}(\xi_{dev}, \hat{\xi}_\beta, v, \delta) \right) = \frac{v^2\, \cos(\tilde{\theta} + \hat{\beta}^R)\, \cos(\hat{\beta}^R)}{L\, \cos^2(\delta + \hat{\beta}^F)} \tag{12}$$

and the quantity in (12) cannot be null since angular deviation, steering angle and sideslip angles never reach $\frac{\pi}{2}$. As a result, sideslip angles estimation $\hat{\xi}_\beta$ obtained thanks to the observer (3) and the functions (7) converges to the unknown actual sideslip angles without direct measurement and can then be used for control purpose.

## IV. Control law

As soon as a relevant estimation of the sideslip angles $\beta^F$ and $\beta^R$ is available, the motion model (1) is fully known and a control law may consequently be proposed, accounting for bad grip conditions. The proposed control approach independently considers lateral and longitudinal dynamics. This is made possible thanks to a preliminary conversion of model (1) into a chained form.

### A. Lateral dynamic control [steering angle]

Let us first consider the lateral servoing. The objective is to find a steering angle control law ensuring the convergence of the angular deviation $y$ to some set point function $y_d(t)$ (i.e. the desired lateral offset may be time-varying). As it has been demonstrated in [8], the model (1) may be turned into a chained form using the state and control reversible transformation (13).

$$\begin{array}{rcl} [s, y, \tilde{\theta}] & \rightarrow & [a_1, a_2, a_3] = \left[ s, y, (1 - c\, y) \tan(\tilde{\theta} + \beta^R) \right] \\ [v, \delta] & \rightarrow & [m_1, m_2] = \left[ \frac{v \cos(\tilde{\theta} + \beta^R)}{1 - c(s)\, y}, \frac{da_3}{dt} \right] \end{array} \tag{13}$$

Moreover, in order to obtain a closed loop behavior independent from velocity $v$, the derivatives with respect to time are replaced in the following by derivatives with respect to the curvilinear abscissa $s$. Let us denote by $a_i'$, $i \in \{1,2,3\}$ the derivative of variable $a_i$ with respect to curvilinear abscissa: $a_i' = \frac{da_i}{ds}$. The motion model (1) then becomes:

$$\left\{ \begin{array}{lcl} a_1' & = & 1 \\ a_2' & = & a_3 \\ a_3' & = & \frac{da_3}{ds} = \frac{m_2}{m_1} \triangleq m_3 \end{array} \right. \quad (14)$$

The motion model (14) is linear, the first state variable $a_2$ is directly the lateral deviation $y$ and the control variable $m_3$ is related to the steering angle $\delta$. The objective then becomes to ensure the convergence of $a_2$ to any set point function $y_d(t)$. Defining the error $\varepsilon_y = y - y_d(t)$, the virtual control $m_3$:

$$m_3 = -K_d\,\varepsilon_y' - K_p\,\varepsilon_y + y_d''(s) \quad (K_d, K_p > 0) \quad (15)$$

allows the convergence of $\varepsilon_y$ to 0 since this virtual control leads to the following differential equation with respect to $\varepsilon_y$:

$$\varepsilon_y'' + K_d\,\varepsilon_y' + K_p\,\varepsilon_y \;=\; 0 \quad (16)$$

The reverse of transformation (13) finally permits to find the control law (17) which ensures the differential equation (16). As a result, as soon as sideslip angles are correctly known, the convergence of $\varepsilon_y$ to 0 is imposed by the steering angle with a settling distance defined by the gains $(K_d, K_p)$, whatever the velocity.

$$\delta = \arctan\left[\tan(\hat{\beta}^R) + \frac{L}{\cos(\hat{\beta}^R)}\left(\frac{c(s)\cos\gamma}{\alpha} + \frac{A\cos^3\gamma}{\alpha^2}\right)\right] - \hat{\beta}^F$$

$$\text{with:} \left\{ \begin{array}{lcl} \gamma & = & \tilde{\theta} + \hat{\beta}^R \\ \alpha & = & 1 - c(s)\,y \\ \eta & = & \tan\gamma - \dfrac{\dot{y}_d(t)}{v\,\cos\gamma} \\ A & = & -K_p\,\varepsilon_y - K_d\,\alpha\,\eta + c(s)\,\alpha\tan^2\gamma \end{array} \right. \quad (17)$$

### B. Longitudinal control [velocity]

The longitudinal servoing aims to impose a possibly varying desired curvilinear distance (denoted $d(t)$ in Figure 1) between the leader and the considered robot (i.e $s_L - s \to d(t)$). By denoting $\varepsilon_s = s_L - s - d(t)$, the objective is to derive a control law for the robot velocity $v$ allowing the convergence of $\varepsilon_s$ to zero. Let us consider its time derivative and the expression of $\dot{s}$ obtained in (1):

$$\dot{\varepsilon}_s \;=\; v_L - v\frac{\cos(\tilde{\theta}+\beta^R)}{1-c(s)\,y} - \dot{d}(t) \quad (18)$$

where $v_L = \dot{s}_L$ is the leader's velocity. Since the observer (3) accurately estimates the rear sideslip angles $\hat{\beta}^R \approx \beta^R$, the control expression (19) ensures the desired convergence.

$$v \;=\; \frac{1-c(s)\,y}{\cos\left(\tilde{\theta}+\hat{\beta}^R\right)}\left(v_L + K_l\,\varepsilon_s - \dot{d}(t)\right) \quad (19)$$

with $K_l$ a positive scalar, homogeneous to the closed loop settling time. Indeed, injecting (19) into the error dynamics (18) leads to the differential equation:

$$\dot{\varepsilon}_s \;=\; -K_l\,\varepsilon_s \quad (20)$$

This shows the exponential convergence of the curvilinear abscissa of the robot to the desired longitudinal distance $d(t)$ from the manually driven vehicle along the trajectory it has achieved. The control law (19) exists providing that $(\tilde{\theta} + \hat{\beta}^R) \neq \frac{\pi}{2}$. It has to be satisfied in practice as soon as the robot is properly initialized. Since the lateral behavior has been made independent from the velocity thanks to derivatives with respect to the curvilinear abscissa, the control laws (17) for the steering angle and (19) for the velocity can achieve the tracking of a manually driven vehicle in lateral and longitudinal axis independently.

## V. Experimental results

### A. Experimental testbed

The proposed adaptive control strategy, relying on a robust estimation of grip conditions, has been tested through full scale experiments using the two mobile robots depicted in Figure 2. Both are electrical, four wheel drive and equipped with two independent steering axles (front and rear). They are able to move up to 4 $m.s^{-1}$. In the framework of this paper, only the second robot is autonomously controlled with the laws (17) and (19), respectively for the front steering wheels and the velocity (the rear steering actuator is here unused). The first robot is remotely controlled. However, any manually driven vehicle could have be used instead, provided that it is able to know its successive positions and send them to the autonomous follower.

Both vehicles are then equipped with RTK-GPS, settled

Fig. 2. Experimental platform

straight up the middle of the rear axle, providing a 2cm-accuracy at 10Hz. They are linked by wireless communication. The follower may then access in real time to the successive positions of the first vehicle (constituting the $\Gamma$ path) and to its velocity $v_L$. Together with its own location, all the state may be known in the Frénet frame: $[s, y, \tilde{\theta}]$.

### B. Observer results

As one of the main contributions of this paper lies in a new observer for sideslip angles, robust at low speed, let us first consider the tracking of the path depicted in Figure 3, with a defined velocity profile crossing zero. In order to

allow the analysis of observer capabilities, this path has been followed three times with the same robot, in three different configurations:

1. Using rolling without sliding assumption: in this case $(\hat{\beta}^F, \hat{\beta}^R) = (0, 0)$ in the control laws, reflecting the classical assumption used in mobile robot control. Results related to this trial are depicted with blue plain line in the following figures
2. Using the CBO observer, previously developed for path following control [4]. As mentioned in section III-A, the inverse of the velocity is used in observer equations. Consequently, in order to enable the robot to stop, this observer is stopped below $0.5m.s^{-1}$. In addition, in order to avoid inconsistent values when the observer is restarted, a Butterworth filter has been set on estimated sideslip angles. Results are shown in blue dashed line in the following.
3. Using the observer (3) proposed in this paper, fed back with the functions (7). Results appear in green dashed-dotted line in forthcoming figures.

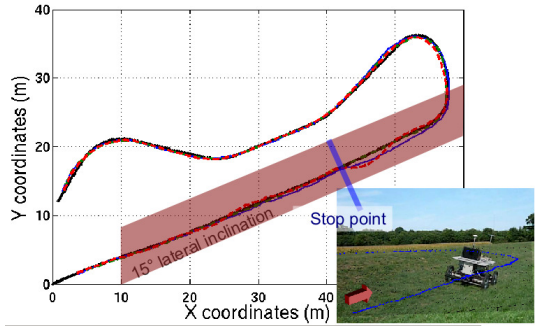


Fig. 3. Reference path and actual trajectories comparison

The reference path $\Gamma$ shown in black line in Figure 3 has been recorded partially on a sloping field and partially on a flat ground (both on grass ground). It is composed of a long straight line with a lateral inclination followed by a long curve and several successive turns. The desired velocity profile is constant (equal to $3m.s^{-1}$) except at the stop point, where a step at a null velocity is imposed during $5s$ (an illustrating video of trial 3 has been submitted with this paper). The desired lateral deviation also stays constant and equal to zero.

Trajectories obtained during the 3 trials are reported in

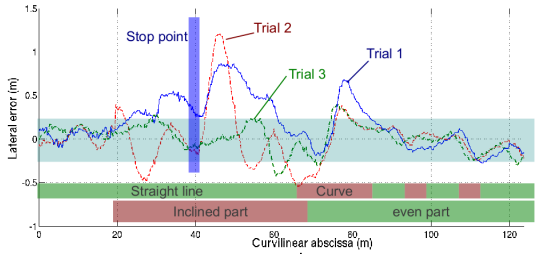


Fig. 4. Comparison of tracking errors

Figure 3, while the tracking errors are compared in Figure 4. First, during the straight line on slope, the bad grip conditions at the considered speed make the robot drifts. As a result, when sliding is neglected, the control law cannot preserve the accuracy and the robot lateral deviation converges to 0.5m (as conditions are roughly constant, up to curvilinear abscissa 40m). After the stopping period (at 40m), the robot tracking error increases during the acceleration (up to 0.8m at 50m) and the robot is only able to come back to the trajectory when the lateral inclination reaches zero (at 65m). The same phenomenon may be noticed during important curves (principally at 78m here, where the error reaches 0.65m), as turning rate generates sliding effects too. In contrast, when sideslip angles are considered (trial 2 and 3), the robot is able to stay on the desired trajectory despite the sliding effects encountered when moving on slope (errors reach zero before and after 40m).

Nevertheless, error dynamics are slightly different during the slope. Before the stop point (at 40m), the previous sideslip angles estimation method is indeed less stable and some oscillations appear during trial 2, while the error stays close to zero during trial 3. However, the main influence of the estimation strategy on the robot control may be observed when stopping the robot. When using the observer defined in [4], the sideslip angles are irrelevant at low speed (due to the division by the velocity) and an important deviation is noticed when the robot is restarted (1.2m at curvilinear abscissa 50m). On the contrary, the performances of the proposed observer are not depreciated at low speeds. As a result, the tracking accuracy is preserved whatever the speed and always stays within $\pm$15cm.

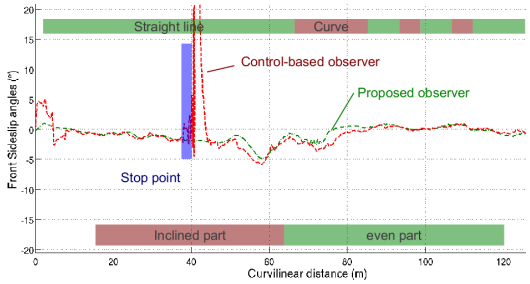


Fig. 5. Comparison of sideslip observation strategy

Figure 4 compares the sideslip angles observed with the proposed strategy to the values supplied by the CBO during the same trial 3. When the robot restarts (at 40m), since the velocity is low and the measurements are noisy, and despite the use of a Butterworth filter, the CBO observer may deliver inconsistent large values for the sideslip angles, as it can be noticed in Figure 4. On the contrary, the observer function (7) is able to supply relevant values when the velocity is close to zero. This explains the difference in tracking errors at 40m between trials 2 and 3. In contrast, when the velocity is significantly different from 0 (and after stabilization), behaviors are quite similar.

### C. Autonomous tracking of a manually driven vehicle

Contrarily to conventional approaches, the proposed control strategy permits to account for bad grip conditions encountered in off-road context, without any restriction on

velocity. As a result, it can be used for tracking a moving target at a desired distance and achieving any motion, including being stopped. In order to demonstrate these capabilities, the control laws (17) and (19) have been used in the configuration depicted in Figure 2, with a null desired lateral offset (i.e. $y_d(t) = 0$) and a 8m longitudinal distance (i.e. $d(t) = 8$).

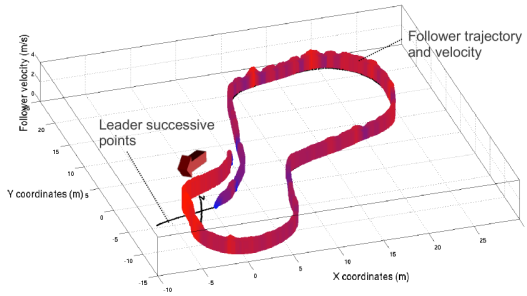


Fig. 6. Leader and Follower trajectory and Follower speed in Z-axis

The trajectory achieved from a remote control of the first vehicle is reported in black line in Figure 6, while the motion of the automatically controlled follower is reported in 3-D, the Z-axis showing the follower velocity. As can be seen on the video submitted with this paper, the leader has a varying speed and even stops, explaining the varying speed of the follower to preserve the longitudinal distance. It can be checked in Figure 6 that the leader trajectory is satisfactorily tracked. In order to be more precise, tracking errors $\varepsilon_y$ and $\varepsilon_s$ are reported in Figure 7, respectively in green plain line and blue dashed line. It can be noticed that the lateral and

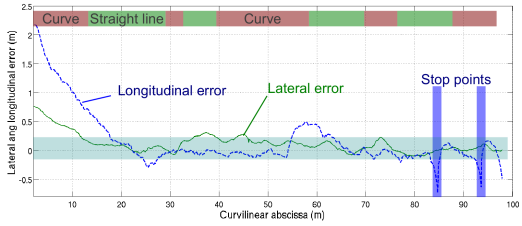


Fig. 7. Lateral and longitudinal error recorded during leader tracking

longitudinal distances are quite accurate after a 15m settling distance. Since the proposed observer is robust with respect to the velocity variations, the lateral error is not affected by the stop points at 85m and 95m. Despite bad grip conditions (the robot moves on wet grass, on the terrain depicted in Figure 2), only small overshoots are recorded at 35m and 75m, when short but quick curves are to be tracked. These overshoots are mainly due to the neglected settling time of the steering actuator. For the same reason, some overshoots are also recorded in the longitudinal error at curvilinear abscissæ 58m, 85m and 95m. They are mainly due to the fast variations in the speed of the manually driven vehicle. In particular, the two stop points are not anticipated by the follower and the settling time in the wheel engines generates these two deviations.

## VI. Conclusion

This paper proposes a control strategy in order to track a moving target with a mobile robot in an off-road context. In this framework, the bad grip conditions together with the target motion and the terrain geometry do not permit to use classical assumptions such as rolling without sliding. A model-based adaptive approach is here proposed in order to estimate on-line and compensate for the influence of sliding effects on the robot behavior. The adaptation law proposed in this paper is not subject to any existence conditions related to the robot velocity. This original point permits to achieve a relevant estimation of the sideslip angles, even when the robot has to stop. As a consequence, an on-line adapted model preserving a kinematic structure is available. It permits to derive independently control laws dedicated to longitudinal and lateral dynamics, acting respectively on the velocity and the steering angle of the robot. As it is pointed out thanks to actual experiments, such a control strategy permits to preserve a high level of accuracy, with respect to disturbing phenomena encountered in natural environments. In particular, the errors encountered when neglecting sliding, occurring mainly during slope or bends are compensated, even when robot has to stop and restart.

As it can be seen on actual tracking results, the accuracy may be depreciated during fast transitions (velocity variations from longitudinal point of view and turning radius modifications from lateral point of view). As it can be checked on simulations, this is mainly due to the neglected settling time and delays of the actuators. If the errors are not significant at low speed, the tracking at higher speed may increase such phenomena. Future work is focused on the integration of predictive algorithm to anticipate for delays and preserve the accuracy even when robot may be subjected to large velocity variations.

## References


[1] B. d' Andréa-Novel, G. Campion, and G. Bastin. Control of wheeled mobile robots not satisfying ideal velocity constraints: a singular perturbation approach. *International Journal of Robust and Nonlinear Control*, 5(4):243–267, 1995.

[2] S. Blackmore, B. Stout, M. Wang, and B. Runov. Robotic agriculture - the future of agricultural mechanisation? *5th European Conference on Precision Agriculture (ECPA), Upsala (Sweden)*, 2005.

[3] G. Campion, G. Bastin, and B. d' Andréa-Novel. Structural properties and classification of kinematic and dynamic models of wheeled mobile robots. In *Ieee international conference on robotics and automation*, pages 462–469, Atlanta, Georgia (USA), 1993.

[4] C. Cariou, R. Lenain, B. Thuilot, and P. Martinet. Adaptive control of four-wheel-steering off-road mobile robots: Application to path tracking and heading control in presence of sliding. In *IEEE/RSJ International Conference on Intelligent Robots and Systems (IROS)*, pages 1759–1764, Nice, France, 2008.

[5] B. Innocenti, P. Ridao, N. Gascons, A. El-Fakdi, B. Lopez, and J. Salvi. Dynamical model parameters identification of a wheeled mobile robot. In *IFAC/EURON symposium on intelligent autonomous vehicles*, Lisboa, Portugal, 2004.

[6] Chang Boon Low and D. Wang. Robust path following of car-like WMR in the presence of skidding effects. In *IEEE international conference on mechatronics*, pages 864–89, 2005.

[7] Pascal Morin and Claude Samson. Motion control of wheeled mobile robots. In *Springer Handbook of Robotics*, pages 799–826. 2008.

[8] C. Samson. Time-varying feedback stabilization of car-like wheeled mobile robots. *International Journal of Robotics Research*, 12(1):55–60, 1993.

[9] C. Samson and P. Morin. Practical and asymptotic stabilization of chained systems by the transverse function control approach. *SIAM Journal on Control and Optimization*, 43(1):32–57, 2005.